buildings

MDPI

Article

Analysis of Power Enhancement in Facade-BIPV Systems Through Module-Level Power Optimizer: Evaluating Performance Under Shading Conditions

Jiyoung Eum [1,2] and Hyun-Jung Choi [1,*]

[1] Department of Building Energy Research, Korea Institute of Civil Engineering and Building Technology, Goyang 10223, Republic of Korea; eumjiyoung@kict.re.kr
[2] Department of Energy Grid, Sangmyung University, Seoul 03016, Republic of Korea
* Correspondence: mingineu@kict.re.kr; Tel.: +82-31-910-0691

Abstract: To combat climate change and achieve global carbon neutrality, photovoltaic (PV) systems have been widely used in the building sector, particularly in zero-energy buildings. In urban areas, space constraints make building-integrated photovoltaic (BIPV) systems appealing, as they combine building materials with power generation and are designed with aesthetics in mind. However, BIPV systems are often affected by partial shading from surrounding structures. Moreover, unlike general PV modules, BIPV modules are custom-designed, resulting in poor electrical specifications. To address these challenges, this study developed a new prototype power optimizer for the module-level power electronics used in BIPV systems. The performance of BIPV systems was evaluated without a power optimizer, with a conventional power optimizer, and with the new prototype power optimizer through simulations and experiments under different shading conditions. Compared with the non-optimized system, power optimizers effectively alleviated shading loss and significantly increased the power efficiency, and the prototype power optimizer achieved a 2.8-fold average improvement in efficiency. This confirms the optimizer function in enabling shaded and non-shaded modules to operate independently at maximum power. Although further research is needed, these optimizers can improve BIPV performance and promote zero-energy buildings.

Keywords: building-integrated photovoltaic system; power optimizer; partial shading; urban environment; power efficiency

check for updates

Citation: Eum, J.; Choi, H.-J. Analysis of Power Enhancement in Facade-BIPV Systems Through Module-Level Power Optimizer: Evaluating Performance Under Shading Conditions. *Buildings* **2024**, *14*, 3850. https://doi.org/10.3390/buildings14123850

Academic Editors: Francesco Nocera and Apple L.S. Chan

Received: 14 October 2024
Revised: 27 November 2024
Accepted: 28 November 2024
Published: 30 November 2024

Copyright: © 2024 by the authors. Licensee MDPI, Basel, Switzerland. This article is an open access article distributed under the terms and conditions of the Creative Commons Attribution (CC BY) license (https://creativecommons.org/licenses/by/4.0/).

1. Introduction

Recently, global interest and investment in sustainable building technology have significantly increased. To achieve carbon neutrality, the International Energy Agency presented a roadmap based on new and renewable energy sources, rather than fossil fuels, to transition the global energy sector to a net-zero energy system by 2050 [1]. In particular, building-integrated photovoltaic (BIPV) systems have emerged as a promising solution aligned with the global trend of increasing photovoltaic (PV) capacity [2].

BIPV systems, particularly those integrated into building facades, have become increasingly important in urban environments [3,4]. These systems not only contribute to energy efficiency in buildings but also utilize vertical spaces for power, offering a solution for renewable energy production in densely populated urban areas where roof space is limited [5]. The increasing emphasis on electrification and energy efficiency improvements in the building sector highlights the potential significance of BIPV technologies [6].

However, facade-BIPV systems face unique challenges, primarily owing to shading from surrounding structures and architectural features. Partial shading is related to power losses in PV systems and is particularly important in BIPV systems [7–9]. This mismatch in power production often results in overall system inefficiencies and reduced energy yields. The complex and dynamic nature of urban shading patterns, which are influenced

by vertical installations, neighboring buildings, trees, and even temporary structures, exacerbates these challenges, making the development of innovative solutions crucial for maintaining system performance.

To address these issues, module-level power electronics (MLPE) devices have emerged as a potential solution. These devices operate at the individual module level, enabling each module to perform at its maximum power regardless of the conditions affecting the other modules in the system [10]. MLPE includes microinverters and direct current (DC) power optimizers. Comprehensive studies have demonstrated significant performance benefits of MLPE under partial shading conditions. Based on a PV testbed, the National Renewable Energy Laboratory reported that the application of individual MLPE devices enhanced PV power efficiency by 20–35% compared with that of string inverters [11]. Baumgartner et al. reported a 1.2% improvement in PV power performance with MLPE compared with centralized inverters under shading conditions [12]. Sarwar et al. noted that MLPE generated 25–35% more PV power under partial shading [13]. Although the effectiveness of MLPE application varies significantly based on shading conditions and installation environments, PV power efficiency is evidently improved when MLPE devices are applied.

Additionally, various converter architectures have been extensively studied to optimize MLPE performance in BIPV applications. Ravyts et al. predicted the availability rates that the series inverter would be 13.5%, the microinverter 87.5%, the series power optimizer 78.9%, and the parallel power optimizer 92.3% over a system life of 40 years, assuming that the BIPV system is installed on the building facade [14]. Spiliotis et al. analyzed, through TRNSYS simulation, the efficiency and power loss of a BIPV-integrated converter according to power control by applying a DC/DC converter integrated into BIPV [15]. In relation to the development of DC/DC converters as power optimizers, Sutikno et al. demonstrated voltage gains of up to 15.83 times under partial shading conditions using voltage multiplier and doubler converters [16]. Raj et al. applied soft-switching techniques to zero-voltage transition and single-ended primary-inductor converters and achieved 97.8% efficiency, whereas conventional designs achieved 93.47% [17]. Furthermore, Osmani et al. analyzed maximum power point tracking (MPPT) algorithms and DC/DC converters for BIPV applications and reported that non-isolated buck-boost converters provided higher efficiency (>95%) than isolated converters (91.2%) while maintaining good performance under partial shading [18].

BIPV modules are custom-designed and manufactured in various sizes and colors according to the building design; therefore, their electrical specifications might be low. Power optimizers are available on the market; however, they are difficult to use directly with BIPV module units because they have been designed for general PV modules and strings.

In a preliminary study [19,20], we modified a conventional power optimizer and used it to verify the effectiveness of applying power optimizers to BIPV systems. The experimental validation compared the performance of BIPV systems without power optimizers to those with conventional power optimizers. The results showed that compared with systems without optimizers, BIPV systems equipped with power optimizers exhibited approximately two to three times lower power loss rates under shading conditions of 10–75%. However, the study was limited to analyzing data from a single clear day, and the effect of the power optimizers was found to be insignificant when the shading ratio was either extremely low or extremely high. In addition, the study highlighted the limitations of using general PV module power optimizers for BIPV systems; such power optimizers do not fully account for the unique characteristics of BIPV modules, such as varied sizes, capacities, and colors.

The present study aimed to address the limitations of the preliminary study and develop a more comprehensive solution for BIPV systems. This study focused on developing and evaluating a BIPV-specific power optimizer that can operate effectively under all shading conditions. The study aimed to improve the control algorithm to ensure optimal performance across all shading scenarios, adapt the power optimizer for compatibility with

BIPV modules, and optimize the minimum operating voltage and power settings while minimizing the size and improving the overall efficiency. To achieve these objectives, both simulations and extended experimental validations were employed. Simulations were conducted by adjusting the inputs for systems without a power optimizer, systems with a conventional power optimizer, and systems with a newly developed power optimizer. In contrast, the experiments were performed by imposing shading conditions on systems without a power optimizer and systems equipped with the newly developed power optimizer. The experiments were conducted over an extended period, encompassing both clear and non-clear days, to offer a more robust validation of the performance of the new power optimizer under real-world conditions.

By addressing the unique challenges of BIPV systems and developing specialized power optimization solutions, this study aimed to contribute to the design of more efficient and reliable facade-BIPV systems. The ultimate goal was to promote the adoption of zero-energy buildings and support carbon neutrality goals in urban environments by providing a more effective and versatile power-optimization solution for BIPV systems.

2. Design and Development of Power Optimizers

The design and development of power optimizers for BIPV systems present unique challenges owing to the specific characteristics of BIPV modules. BIPV modules of various sizes are designed to meet the architectural requirements. These modules are often designed to be small in size, and because they have a low capacity with low input and operating voltages, a customized approach to power optimization is necessary. To address these challenges, a prototype power optimizer was developed that can operate with various module capacities while effectively managing low-voltage operations.

The power optimizer system integrates several key components to increase energy efficiency and maintain safety in BIPV installations. To ensure safety, a rapid-shutdown field-effect transistor (RSD FET) was incorporated, enabling quick shutdown in the case of emergencies or faults.

A crucial design choice for this system is the use of a buck converter topology combined with a full-power processing (FPP) approach. A buck converter is employed to decrease the voltage and increase the current, thereby optimizing the power from the PV modules. The use of FPP, where the entire power of the PV module is processed, was dictated by the frequent mismatch conditions encountered in BIPV systems. Although differential power processing, which involves only mismatched power, can be more efficient in systems with occasional mismatches, the constant shading and mismatch issues in urban BIPV installations make FPP a more suitable choice. This approach ensures that the system can maintain optimal MPPT even under consistent mismatch conditions, which is crucial for maximizing the power in BIPV systems.

Figure 1 presents the system topology and block diagram of the newly developed power optimizer. Figure 1a shows the system topology, highlighting the key components and their interconnections within the BIPV power optimization system. Figure 1b shows a detailed block diagram of the power optimizer, demonstrating the specific arrangement and relationships between components, such as the PV module, buck converter, microcontroller unit (MCU), and communication interfaces. Note that although the power optimizers are connected in series with the microinverter, they operate independently without direct communication. Each optimizer performs its own MPPT control at the module level, ensuring optimal performance under varying conditions while maintaining the electrical characteristics of the series connection.

The block diagram (Figure 1b) shows that a dedicated driver manages the operation of both the buck converter and RSD FET. The entire system is coordinated by an MCU, which serves as the central control unit and oversees the power conversion process and the operation of various components. To facilitate effective coordination and control, the system uses power-line communication (PLC) for reliable communication between the components.

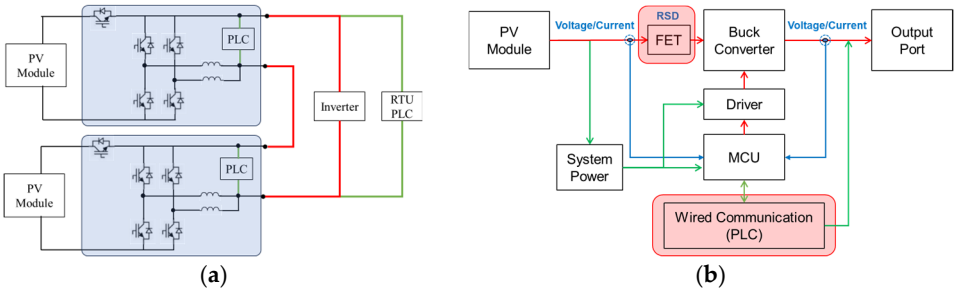

Figure 1. System topology and block diagram of the developed power optimizer for BIPV systems. (**a**) System topology. (**b**) Block diagram.

The control algorithms for the power optimizer were specifically designed to address the unique challenges of BIPV systems by integrating several key features to optimize performance under varying conditions. At the core of the system is the power management integrated circuit (PMIC)-able control, which is implemented in the hardware, establishing a precise voltage threshold for MCU activation. This is complemented by minimum input voltage control, a firmware-based feature that defines the minimum operating voltage condition. Both controls ensure that the system starts and operates only when sufficient power is available, preventing unnecessary energy consumption and system instability under the fluctuating solar irradiance conditions of urban BIPV systems.

The power optimizer operates in four distinct modes—Sleep, Stop, Start, and Run—each of which is tailored to maximize energy efficiency and system performance. The transitions between these modes are based on the input voltage (VPV_IN), input current (IPV_IN), and time conditions (T, T1, T2, and T3). This adaptive-mode switching ensures optimal performance under various environmental conditions. In the Run mode, which is the primary operational mode, the optimizer actively manages power conversion and performs MPPT.

A significant innovation in algorithm design is the decoupling of shading detection control and maximum power point voltage (Vmp) tracking control. This separation enables rapid recovery to the previous Vmp during transient shading events, thus minimizing power loss during intermittent shading, which is common in urban environments. It also enables additional operations for maximum power tracking after Vmp recovery, enhancing the ability of the system to adapt to the dynamic shading patterns that are characteristic of BIPV installations in built-up areas.

The control algorithm illustrated in Figure 2 presents a comprehensive flowchart of the system operation. This dual-control structure is divided into overall operation and run-mode controls and enables both broad system management and fine-tuned power optimization. In the Run mode, the algorithm manages power based on the current power input (PI) relative to the maximum power input (MAX_PI), including regular power scanning (P_SCAN) to check the power state and compare the input power (P_IN) with the MPPT.

The physical design of the power optimizer was carefully considered to ensure seamless integration with existing BIPV installations. Designed to be adjustable in size, the optimizer can fit within various curtain wall frames where BIPV modules are mounted. This flexibility enables easy incorporation into diverse BIPV designs without compromising aesthetics or functionality. Advanced thermal management techniques have been incorporated into the design, ensuring efficient operation even under the high-temperature conditions often encountered in building-integrated systems.

Simulations and experimental tests were conducted to evaluate the performance of the developed power optimizer prototype. These comprehensive evaluations assessed the performance of the optimizer under a range of BIPV operating conditions, with a particular focus on partial shading scenarios. The following sections present the detailed methods and results of these simulations and experiments, providing insights into the effectiveness of the optimizer in enhancing BIPV system performance.

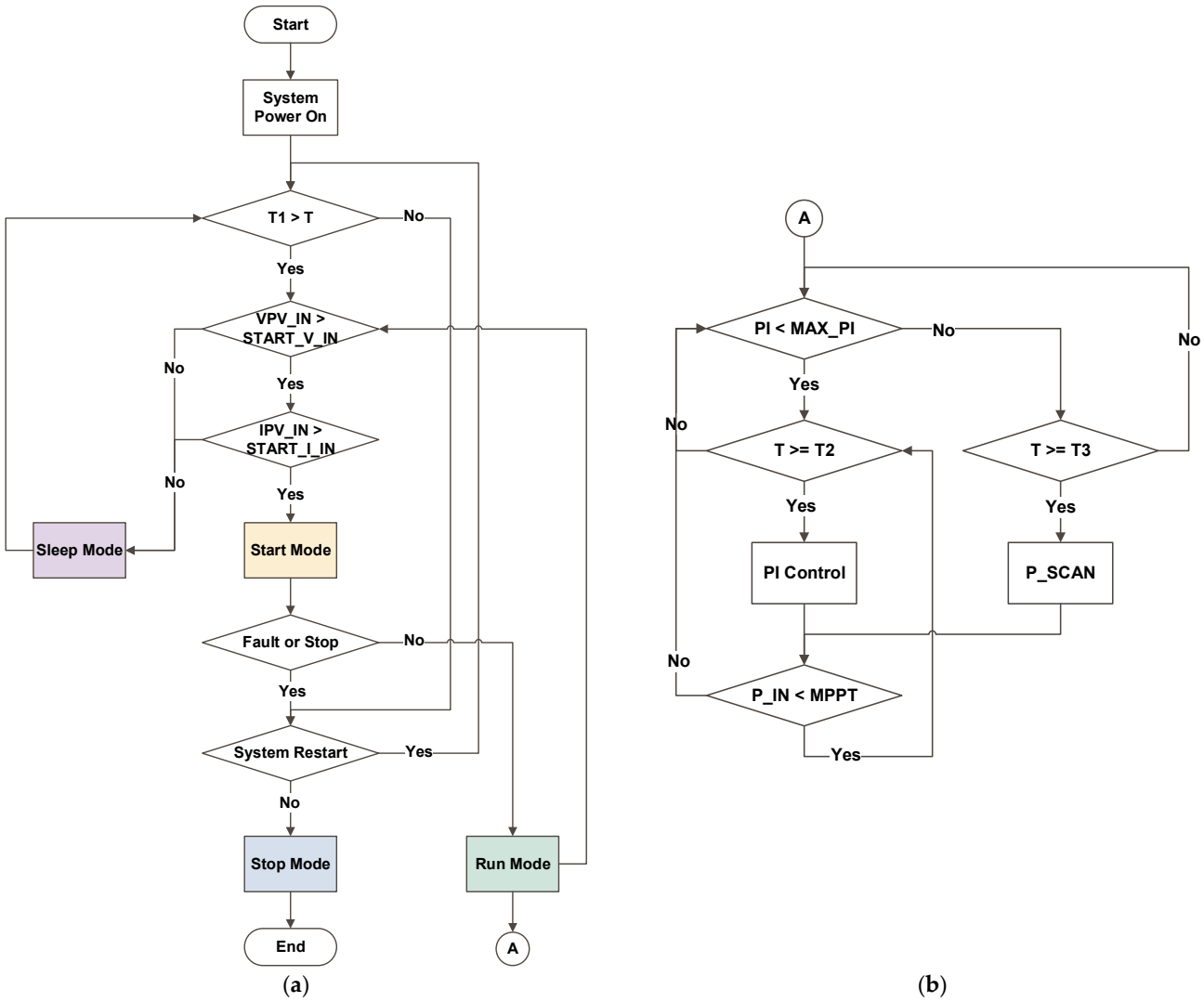

Figure 2. Control algorithm flowchart of the newly developed power optimizer for BIPV systems. (**a**) Operation mode. (**b**) Run mode.

3. Simulation Methods and Results

3.1. Simulation Methods and Settings

This study employed a simulation setup to evaluate the performance of BIPV systems under various conditions by comparing different power optimization strategies. The experimental apparatus, illustrated in Figure 3, was designed to simulate real-world scenarios while enabling the control and measurement of system parameters. Figure 3b shows the new prototype power optimizer used in the simulation setup. A conventional product was also connected in the same manner and simulated for comparison.

The setup included two CHROMA 62100H-600S solar array simulators as PV module simulators. These devices emulated the electrical characteristics of BIPV modules under various environmental conditions. Initially, the simulators were set to over 160 W of power, leading to intermittent inverter errors, which were likely due to the input power limitations of the inverter. To address this issue and ensure stable operation, the maximum power setting of the simulators was adjusted to 105.6 W, which was determined to be the optimal power level for consistent inverter performance without errors. The DC power from these simulated PV modules was fed into a Hansol HSPV-K360 microinverter (capacity: 330 W, MPPT voltage range: 22–52 V) to convert the DC power to AC power.

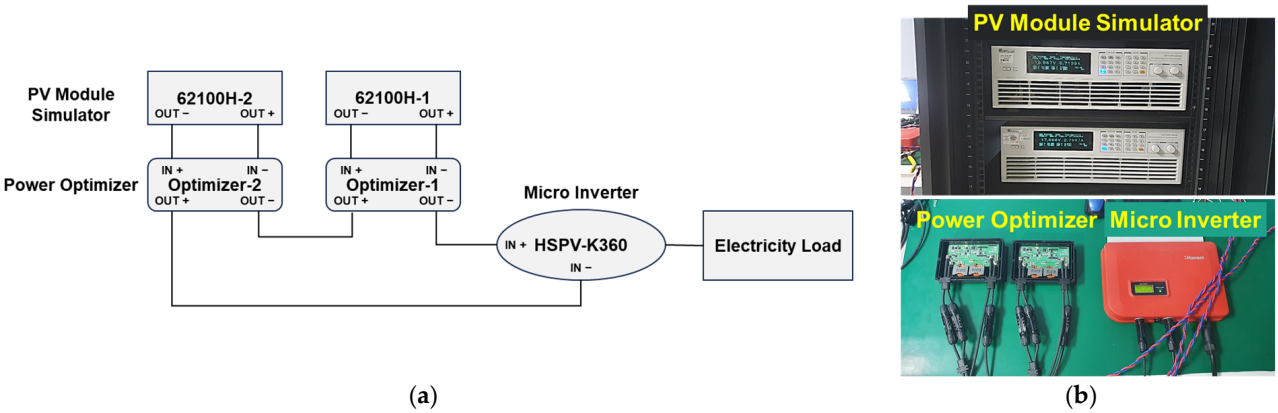

Figure 3. Diagram and pictures of the BIPV system simulation configuration. (**a**) Diagram. (**b**) Pictures.

Three configurations were evaluated: a system without power optimizers, a system with conventional power optimizers (Nanoom Energy NE-GC-02), and a system with prototype power optimizers. The comparison was conducted under identical conditions.

The simulations were conducted using controlled power variations. The power of one PV module in the system was systematically varied to represent the different levels of PV power production. The power levels were adjusted from 100 to 90%, 75%, 50%, and 25% of the rated power. The power was maintained at 300 s (5 min). Data were collected at 100-ms intervals; this frequency was selected to capture rapid fluctuations in power while maintaining manageable data volumes. This high-resolution data collection enabled a detailed analysis of the system response to changing conditions.

3.2. Simulation Results and Analysis

The simulation results revealed distinct performance characteristics among the three tested BIPV system configurations. A power adjustment simulating the shading effect was performed on one module, which also affected the remaining module connected in series without power adjustment, thereby changing the system power.

Figure 4 shows the power of each module and system through the power stages under each condition, depending on the configuration. In this simulation, stepwise power adjustments were applied to simulate varying shading conditions, with power stages set at 100%, 90%, 75%, 50%, and 25% of the rated power. Each step lasted 300 s, allowing the system to stabilize and data to be collected at 100 ms intervals. The *x*-axis in Figure 4 represents the cumulative time across all steps, including the transitions between adjustments. This sequential representation highlights the performance differences among the tested configurations. An adjusted module is a module with an arbitrarily lowered rated output, similar to that in the shade. An unadjusted module is a module whose rated output has not been adjusted separately, as shown by the absence of shade. The system was originally expressed as the output of the BIPV system via an inverter connecting these two modules. When power fluctuates in one module, systems without power optimizers exhibit considerable fluctuations and steep drops in power. The systems with conventional power optimizers demonstrated improved stability, albeit with persistent fluctuations. In contrast, the systems with the prototype power optimizers showed remarkably stable power under all conditions.

Figure 5 shows the power efficiency loss rate based on the MPPT efficiency according to the maximum power ratio. Figure 5a shows the module-level efficiency loss rates for each condition. The green line in Figure 5a represents the power loss rate of the rated output adjustment module according to the installation conditions of the power optimizer in the BIPV system. The power loss rate of the adjusted module for each condition was compared with that of the unadjusted module and was derived as an average value as it showed a

similar level. As the power of one module decreased, the system without power optimizers exhibited similar losses for both modules. Compared with the non-optimized system, the system with conventional power optimizers demonstrated improved performance. However, under excessively low or excessively high shading, the effect was insignificant. The system with the prototype power optimizer exhibited the lowest power loss rate for the modules without any power regulation, maintaining the power loss rate below 6% across all power levels. In particular, under 75% shading conditions, the new optimizer resulted in a power efficiency loss difference of approximately 69.2% compared with that of the non-optimized system. This suggests that the optimized power extraction from each module was effectively isolated.

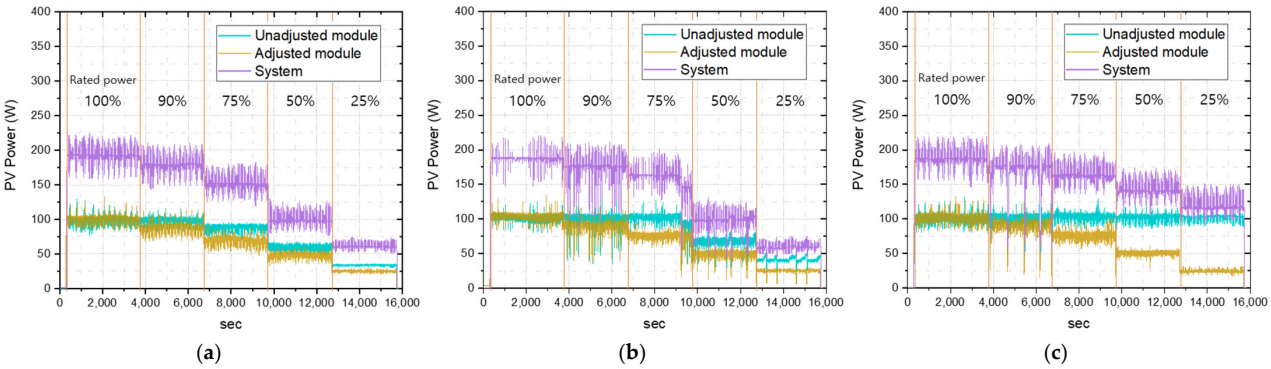

Figure 4. Power comparison of BIPV system configurations under stepwise power adjustments (100%, 90%, 75%, 50%, and 25%) for 300 s. (**a**) Without PO *. (**b**) Conventional PO. (**c**) Prototype PO. (* PO: power optimizer).

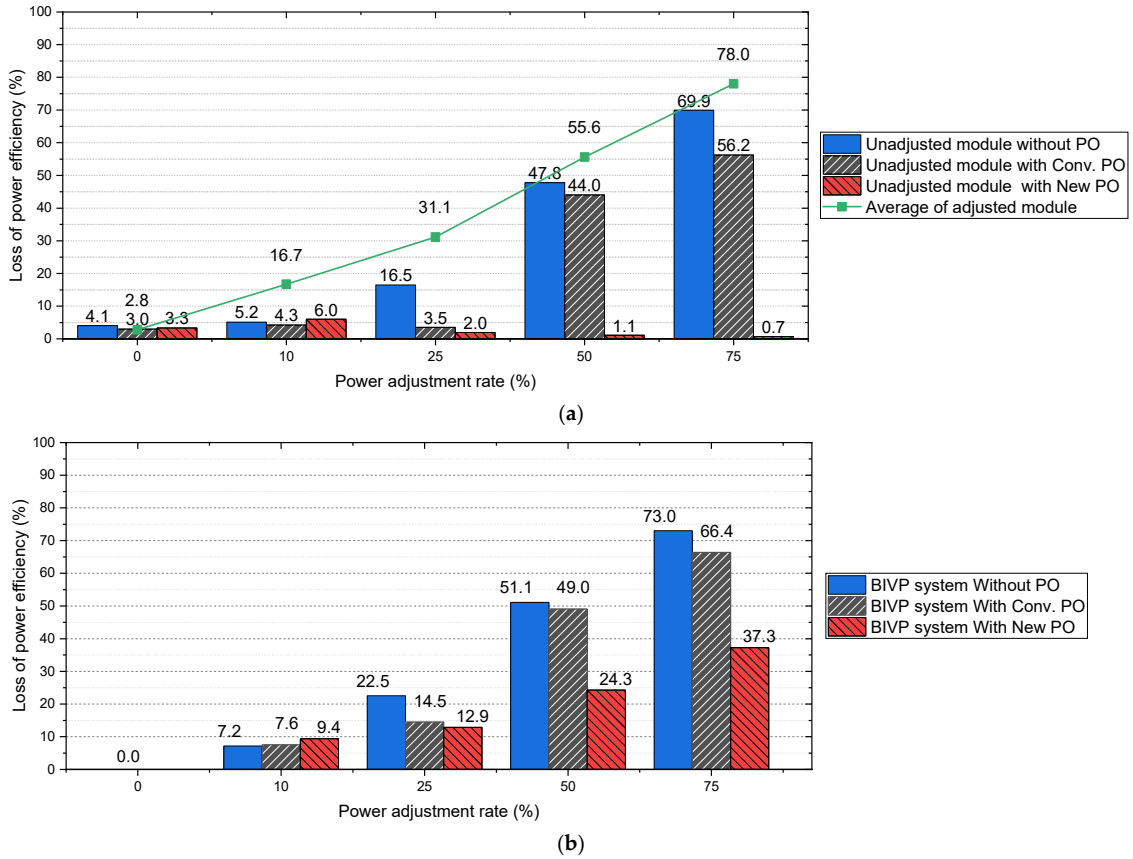

Figure 5. Efficiency loss rates at the module and system levels for different BIPV configurations. (**a**) Module-level. (**b**) System-level.

Figure 5b shows the system-level power-efficiency loss rate. The effect of the power optimizers became significant at a 25% power reduction, with the difference between the conventional and prototype power optimizers becoming apparent at 50% reduction and above. At 75% power reduction, the system without optimizers showed a 73.0% loss rate, the conventional optimizer system showed a 68.4% loss rate, and the prototype power optimizer system showed a loss rate of only 37.3%. The average power efficiency loss rate through each power adjustment was calculated to be 30.8% for the non-installed power optimizer, 27.5% for the conventional power optimizers, and 16.8% for the prototype optimizer.

Owing to its higher power performance, the prototype power optimizer outperformed both the non-optimized and conventionally optimized systems. This high efficiency, maintained even at low power, suggests the possibility of preventing system power loss through isolated power optimization for each module, although the shading or reduced power of one module can significantly impact the system. The superior performance of the prototype power optimizers can be attributed to their advanced MPPT algorithms and ability to operate effectively at lower voltage levels, which are common in partially shaded BIPV modules.

4. Experimental Methods and Results

4.1. Experiment Methods and Settings

The experimental location was an office building in Goyang-si, Gyeonggi-do, South Korea. In this comparative study of two BIPV systems, a variety of specialized materials and equipment were utilized, as shown in Figure 6. The core components of each system were BIPV modules manufactured by KOES, each producing 171 W of power (maximum output voltage of 20.77 V) with an efficiency of 12.2%. These modules featured a single-crystal silicon construction with a glass-to-glass design incorporating 36 cells and a dark gray color. A notable aspect of the system without power optimizers was the series connection of two modules of different lengths, with one module extending 30 cm beyond the other. Owing to its consistent cell structure, this configuration resulted in varying power efficiencies when calculated based on the module area despite identical electrical specifications. In the experiment, two sets of BIPV systems were used, each with two BIPV modules connected in series. Therefore, four BIPV modules were used. One set had no power optimizer installed, and the other set had two new power optimizers installed on each of the two modules. Because one set of BIPV systems comprised two modules connected in series, the rated capacity was 342 W. Figure 7 shows a schematic of the experimental apparatus. A comparison with the conventional power optimizer was performed through simulation, whereas an experimental comparison of the non-installed system and conventional power optimizer system was performed in prior research by Eum et al. [20].

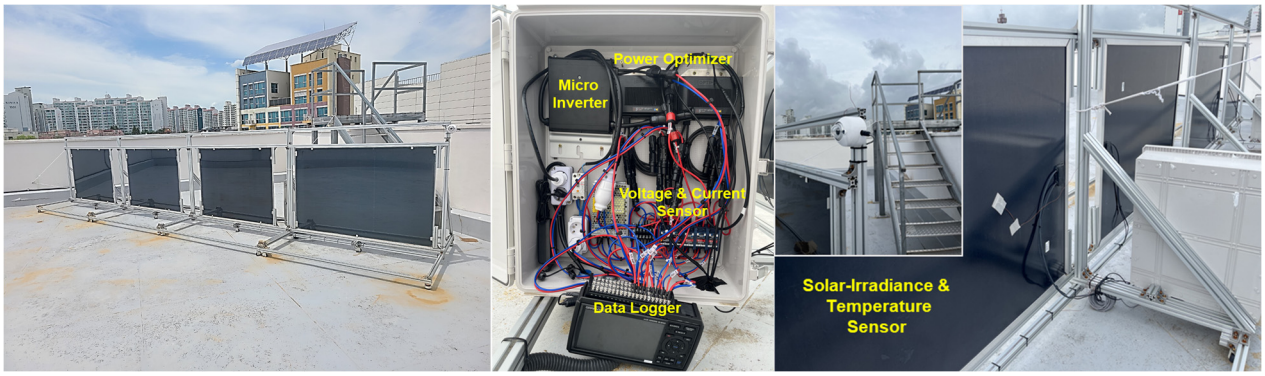

(**a**) (**b**) (**c**)

Figure 6. Pictures of the experimental apparatus. (**a**) Front side. (**b**) Device box. (**c**) Solar irradiance and temperature sensor.

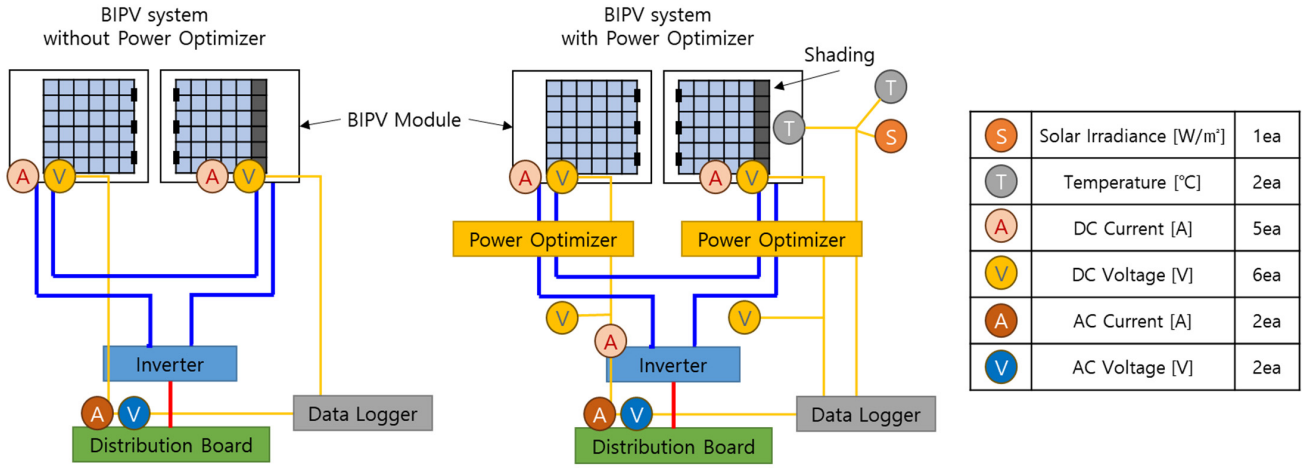

Figure 7. Schematic of the experimental apparatus used to compare BIPV systems without optimizers and with the newly developed prototype power optimizers.

The systems employed MI-350 microinverters from Hoymiles, each with a capacity of 350 W (input voltage range of 16–60 V) and minimum efficiency of 94.79%. Owing to the spatial constraints at the experimental site, which limited the number of modules that could be installed, one inverter was used per system. The small capacity of these arrays necessitated the use of microinverters instead of conventional small-capacity inverters. The prototype power optimizer had a capacity of 600 W and an MPPT voltage range of 8–60 V, and it was installed for each module in one of the two BIPV systems. The experimental equipment consisted of a microinverter and power optimizer with low input and operating voltages, considering the experimental environment and BIPV module.

The solar irradiance was measured using an EKO MS-60 m positioned at a 90° angle to match the inclination of the BIPV modules. The temperature was measured using TC-T thermocouples placed on both the top and rear of the module to record the air and module temperatures. All the data were logged using a GRAPHTEC midi LOGGER GL840 connected to a solar irradiance meter and thermocouple. The measurement accuracy of the solar irradiance meter was ±1%, and that of the data logger was ±0.5%.

For data acquisition, the study employed transformers from Seri2B. The current transformer (model ICT-D4) and voltage transformer (model IVT-D4) provided dual-power signals of DC 0–5 V and 4–20 mA. These transformers were used to measure and monitor the electrical parameters and were connected to a data logger. All pieces of equipment were certified by Korean Industrial Standards. The experimental error was estimated to be approximately ±1.6%, which was calculated using a transformer (±0.5%), an irradiance meter, and a data logger. The data collection period spanned from 25 July 2024, to 11 September 2024, with measurements taken at 1 min intervals. Unlike in simulations, in actual experiments, measurement intervals shorter than 1 mi can result in high noise in real-time measurement data, and data may be lost during storage. Therefore, an interval of 1 min was set to ensure data reliability.

Opaque sheets were used to simulate the shading conditions. Based on the front view, the module located on the right side of each array was shaded to create consistent shading. The partial shading condition was implemented at area ratios of 10%, 25%, 50%, and 75% for one module of each BIPV system. Because the cells within the module were connected in series, shading was uniformly applied across the module, considering the cell area. The shading was maintained during the experimental period of each condition. This approach enabled a comparison of the system performance under partial shading conditions.

4.2. Experimental Results and Analysis

The analysis of the BIPV power relative to the daily solar irradiance focused on clear days with a mean cloud cover of three or fewer for each shading condition. Weather

information for this region was provided by the Korea Meteorological Administration [21]. Table 1 lists the daily operating characteristics of BIPV systems with and without power optimizers. The daily maximum power values within parentheses are the power efficiencies calculated based on a rated power of 342 W, and the daily energy values within parentheses express the power performance. Owing to the vertical installation of BIPV modules, the maximum power efficiency was less than 50% and decreased with increasing shading ratio. The performance ratio (PR) was used to evaluate the power performance of the system. The PR was calculated using Equation (1), and the actual power of the BIPV system was compared with the theoretically calculated power. Expressed as a percentage, the PR considers the relative efficiency of the vertical solar irradiance and the BIPV system. Systems equipped with power optimizers showed a reduced decrease in power performance, and this effect became more pronounced with increasing shading ratio.

Table 1. Daily operating characteristics of BIPV systems with and without power optimizers under different shading conditions.

Shading Condition	Date	Mean Cloud Amount/d	Maximum PV Power (W)		PV Energy (kWh/d)	
			Without PO *	With New PO	Without PO	With New PO
No shading	4 August 2024	2.5	153.88 (45.0%)	148.53 (43.4%)	1.08 (91.7%)	0.98 (90.2%)
Shading 10% on 1 module	9 August 2024	2.8	155.90 (45.6%)	148.47 (43.4%)	0.86 (89.1%)	0.87 (91.9%)
Shading 25% on 1 module	16 August 2024	3.0	145.20 (42.5%)	134.74 (39.4%)	0.69 (74.6%)	0.70 (77.6%)
Shading 50% on 1 module	28 August 2024	0.4	105.00 (30.7%)	128.79 (37.7%)	0.66 (52.8%)	0.78 (64.0%)
Shading 75% on 1 module	10 September 2024	1.3	64.33 (18.8%)	113.51 (33.2%)	0.34 (27.4%)	0.65 (54.0%)

* PO: power optimizer.

Previous studies have analyzed the effects of conventional power optimizers only on specific clear days. When daily data were compared across different shade conditions, the impact of conventional power optimizers was insignificant at very low or high shading ratios. However, the newly developed prototype power optimizer used in the current study demonstrated the ability to prevent power loss across all shading conditions.

$$PR = \frac{\sum P_{measured,i} \times \Delta t}{\sum P_{calculated,i} \times \Delta t} \times 100\ [\%] \quad (1)$$

where

$$P_{measured,i} = \text{Measured power output at } i \text{ min [kW]}$$

$$P_{calculated,i} = \text{Calculated power output at } i \text{ min} = G_i \times (A_1\eta_1 + A_2\eta_2) \times \eta_{inv}[\text{kW}]$$

$$G_i = \text{Solar irradiance at } i \text{ min } \left[\text{kW}/m^2\right]$$

$$A_1, A_2 = \text{Area of each module type } \left[m^2\right]$$

$$\eta_1, \eta_2 = \text{Efficiency of each module type}$$

$$\eta_{inv} = \text{Inverter efficiency}$$

$$\Delta t = 1/60\text{h}$$

Figure 8 shows the daily 1 min power and solar irradiance on a specific, clear day under each shade condition. As the shade ratio increased, the systems with power optimizers consistently outperformed those without power optimizers. Consistent with the simulation

results, the systems exhibited larger power differences near noon when the power was high than in the early morning and late afternoon hours when the power was lower.

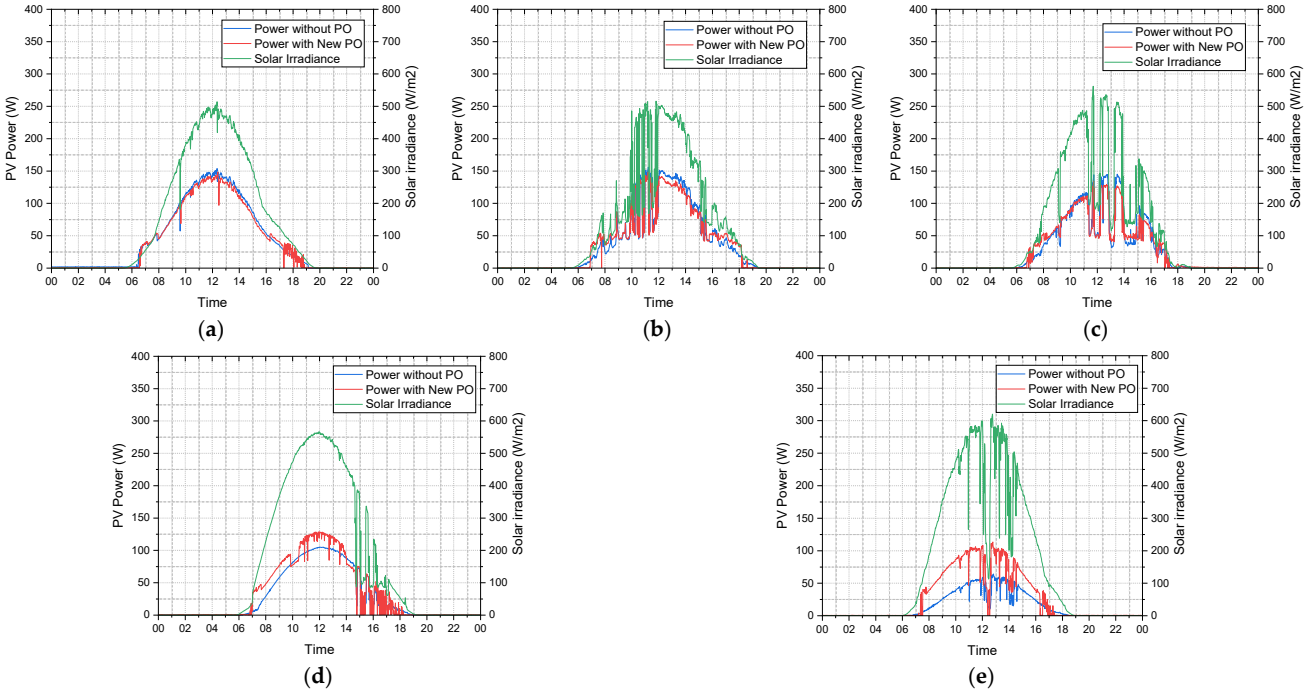

Figure 8. Daily PV power and solar irradiance of BIPV systems under different shading conditions. (**a**) No shading, 4 August 2024. (**b**) Shading 10% on 1 module, 9 August 2024. (**c**) Shading 25% on 1 module, 16 August 2024. (**d**) Shading 50% on 1 module, 28 August 2024. (**e**) Shading 75% on 1 module, 10 September 2024.

Figure 9 shows the changes in voltage, current, and power for a BIPV system when one module was subjected to 75% shading, comparing scenarios with and without power optimizers. Without power optimizers, the voltages and currents of both the shaded and non-shaded modules were identical. Under these conditions, the power efficiency of the shaded module was 28.4%, whereas that of the non-shaded module was 27.7%, indicating that the performance of the non-shaded module was severely affected by the shaded module. Conversely, when the power optimizers were installed, the voltage of the shaded module decreased, whereas the current of the non-shaded module increased. Consequently, although the power efficiency of the shaded module slightly decreased to 20.2%, the efficiency of the non-shaded module significantly improved to 92.7%, indicating minimal impact from the shaded module. These changes occurred because the power optimizers individually tracked and optimized the maximum power point of each module. Consequently, in systems with power optimizers, the overall power efficiency improved substantially, even under 75% shading on one module.

The relationship between the PV power and solar irradiance under various shading conditions was analyzed to evaluate the performance of the BIPV systems with and without power optimizers. Figure 10 shows scatter graphs that reveal the patterns of both system types across different shading scenarios. These graphs are based on data collected over a minimum of 5 d for each shading condition, thereby providing a comprehensive representation of the system performance. Both systems demonstrated a positive correlation between solar irradiance and power. As the shading increased from 10% to 75% in one module, the difference in performance between the two systems became more apparent. Figure 10b–e show that the system equipped with a power optimizer maintained a higher power across irradiance levels. In contrast, the system without a power optimizer exhibited a more pronounced decrease in power as the shading intensified. This trend was observed in the 50% and 75% shading scenarios, as depicted in Figure 10d,e.

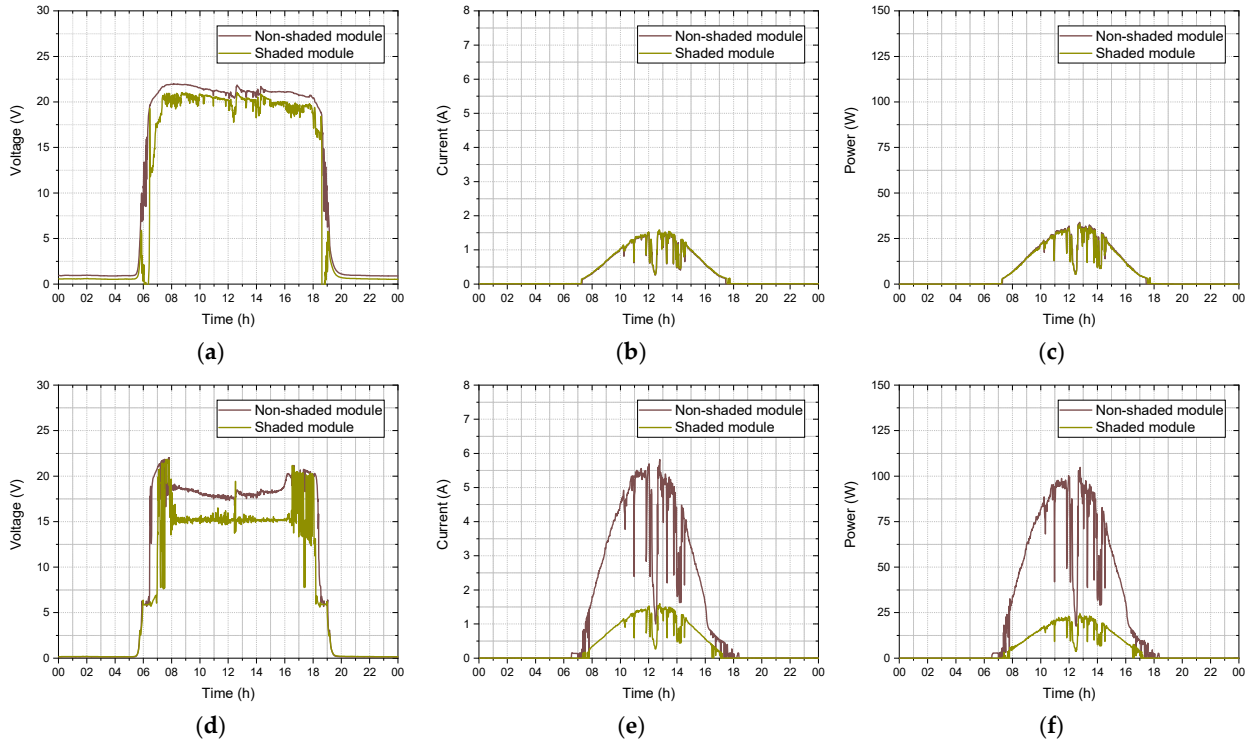

Figure 9. Daily electrical characteristics of a BIPV system under 75% shading with and without power optimizers (10 September 2024). (**a**) Voltage without optimizers. (**b**) Current without optimizers. (**c**) Power without optimizers. (**d**) Voltage with optimizers. (**e**) Current with optimizers. (**f**) Power with optimizers.

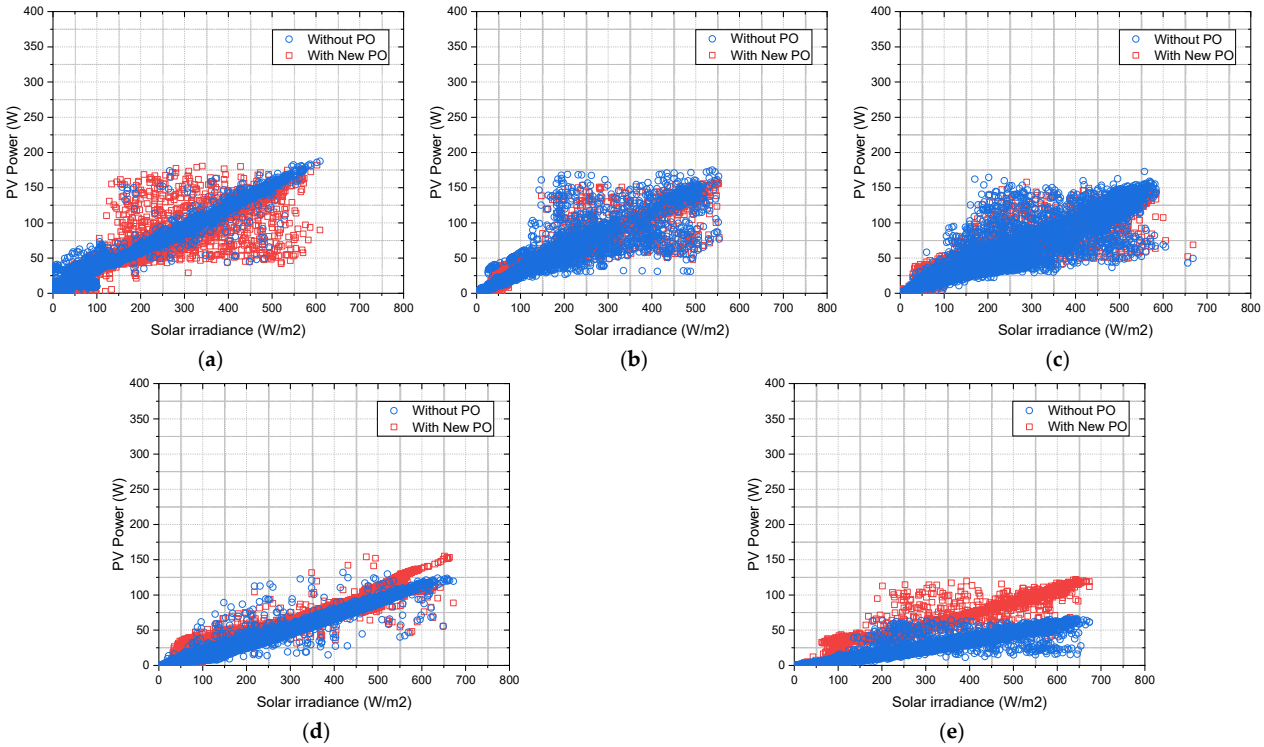

Figure 10. Relationship between PV power and solar irradiance under different shading conditions. (**a**) No shading. (**b**) Shading 10% on 1 module. (**c**) Shading 25% on 1 module. (**d**) Shading 50% on 1 module. (**e**) Shading 75% on 1 module.

Figure 11 presents a linear regression analysis of the PV power and solar irradiance for various shading scenarios. As depicted in Figure 11a, the BIPV system without power optimizers showed a decrease in the slope of the regression lines with increasing shading, indicating a reduction in system efficiency. In contrast, as shown in Figure 11b, the BIPV system with the prototype power optimizers maintained higher slopes across all shading conditions, indicating improved resilience to power losses due to shading.

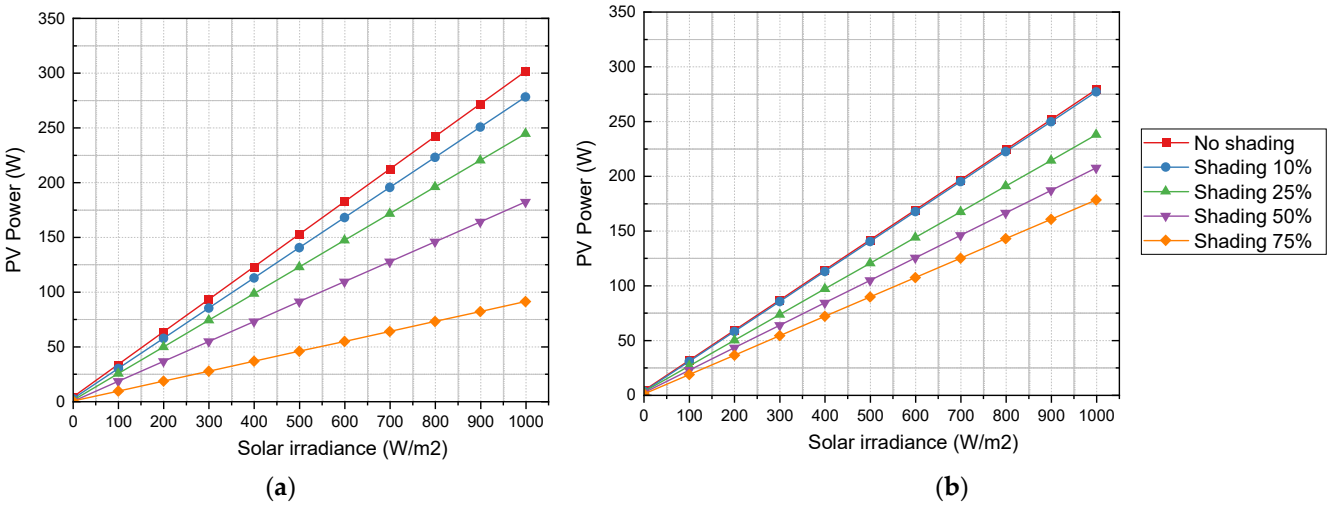

Figure 11. Linear regression of PV power and solar irradiance for shading scenarios. (**a**) BIPV system without power optimizers. (**b**) BIPV system with the prototype power optimizers.

Figure 12 presents a comparison of the BIPV system efficiency losses under various shading conditions, with and without power optimizers. The graph shows the average efficiency loss rates calculated for each shading condition, using the no-shading scenario as a baseline. In the absence of shade, neither system experienced any losses. However, as the shading intensified, the system with the power optimizer consistently demonstrated lower efficiency losses than the system without a power optimizer.

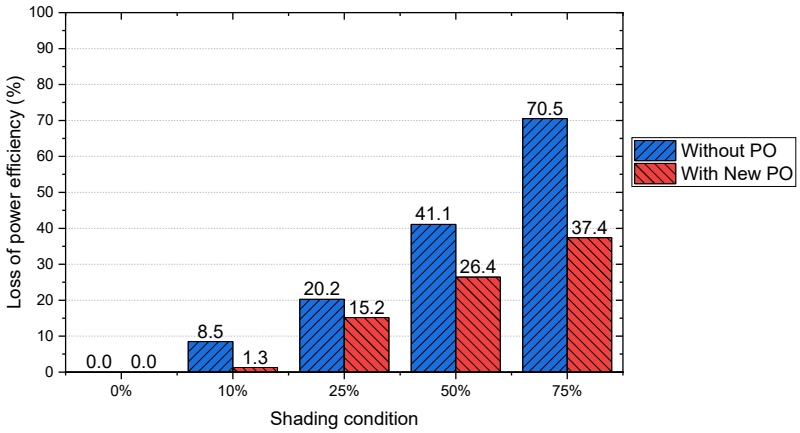

Figure 12. BIPV system efficiency losses under shading conditions with and without power optimizers.

The effectiveness of the power optimizer became more pronounced as the shading severity increased. At 10% shading, the average efficiency loss significantly decreased from 8.5% to 1.3% when the optimizer was used. As the shading increased to 25%, the losses decreased from 20.2% to 15.2%. Under 50% shading, the reduction in losses was more pronounced, decreasing from 41.1% to 26.4%. Finally, under 75% shading, the optimizer facilitated a substantial decrease in losses from 70.5% to 37.4%. This was particularly evident in the 50% and 75% shading scenarios, where the system equipped with the power optimizer maintained significantly higher power than the system without a power optimizer.

These results were derived from data collected over multiple days for each shading scenario, providing a comprehensive representation of the system performance under various conditions. Across all shading conditions, the system with the power optimizer showed an average efficiency loss of 20.1%, whereas the system without an optimizer showed an average efficiency loss of 35.1%.

5. Discussion

The results of both the simulations and experiments provided valuable insights into the impact of partial shading on facade-BIPV systems and the effectiveness of module-level power optimizers in mitigating such effects. In urban environments, facade-BIPV systems are highly susceptible to the shading caused by nearby buildings and structures, which leads to significant power losses. Our study demonstrated that the prototype optimizer can substantially mitigate these losses, achieving a 2.8-fold average improvement in efficiency across all shading conditions compared with non-optimized systems. The efficiency losses were significantly reduced to 1.3% under optimal conditions and were no greater than 37.4% under severe shading.

A key advantage of the prototype optimizer is its ability to decouple the performance of the shaded and unshaded modules. This decoupling enables each module to operate at its own power point, effectively isolating the impact of shading on the individual modules. For example, when one module was subjected to 75% shading, the unshaded module maintained a high efficiency of 92.7%, whereas the efficiency of the shaded module decreased to 20.2%. This significant disparity in performance underscores the effectiveness of power optimizers in mitigating the adverse effects of shading. Furthermore, as the number of connected modules increases, the benefits of the power optimizer are likely to become even more pronounced, thereby enhancing the overall system performance. Consequently, unshaded modules can maintain high efficiency even when other modules in the system are significantly shaded, which is a crucial feature of BIPV systems in urban environments with non-uniform solar irradiance.

Unlike conventional optimizers, which only improved the performance under specific shading conditions, the proposed prototype optimizer consistently prevented power losses across a wide range of shading scenarios. This consistent performance across various shading ratios demonstrated the robustness of the optimizer in real-world urban settings.

6. Conclusions

The main purpose of this study was to address the partial shading issue that reduces the PV power efficiency of BIPV systems in urban environments where shading occurs frequently. Unlike conventional power optimizers designed for standard PV modules, the newly developed prototype in this study was tailored to accommodate the low voltage and small capacity characteristics of BIPV modules. By enhancing both the firmware and hardware, this advanced module-level power optimizer demonstrated improved efficiency and stability, enhancing system performance under various shading conditions.

Compared with non-optimized systems, the prototype system achieved a 2.8-fold improvement in efficiency, with power loss reduced to 1.3% under optimal conditions and limited to 37.4% under severe shading. By isolating the performance of each module, the power optimizer maximizes the output under shading, which would be beneficial in urban facades. This enhances energy efficiency, reduces mismatch losses, and accelerates investment recovery, supporting the feasibility of zero-energy buildings. Although the system involves some additional initial costs, increased complexity, and maintenance requirements, and although the prototype power optimizer may yield similar or slightly lower improvements in efficiency under low shading conditions, these limitations are offset by its consistent performance improvements across all shading conditions through effective module-to-module mismatch minimization.

These results indicate that optimized BIPV systems can contribute to increased practicality and economic feasibility in urban environments by potentially shortening the investment cost recovery period and improving operational profits. Additionally, the ability to independently optimize and monitor the performance of each module enables prompt responses to maintenance needs, which may reduce long-term maintenance costs and support the overall practicality and cost-effectiveness of the system.

Further studies are recommended to assess the potential of optimized BIPV systems in urban environments. These should include long-term performance evaluations under various urban shading patterns, optimization strategies for different BIPV module types, and economic feasibility assessments. Furthermore, comparative performance analyses between conventional power optimizers and the developed prototype in various urban environments are planned to validate the system's practical advantages. The economic analysis should particularly focus on various installation scenarios (single module, multiple modules, strings, etc.) and their associated costs and benefits, including the initial investment and potential returns. These investigations will contribute to enhancing the efficiency, reliability, and applicability of optimized BIPV systems in urban environments.

Author Contributions: Conceptualization, J.E. and H.-J.C.; methodology, J.E. and H.-J.C.; data curation, J.E.; formal analysis, J.E.; visualization, J.E.; writing—original draft preparation, J.E.; writing—review & editing, J.E. and H.-J.C.; supervision, H.-J.C. All authors have read and agreed to the published version of the manuscript.

Funding: This study was conducted under the KICT Research Program (project no. 20240325-001, Research on the Development of a Green Retrofit Package to Improve the Indoor Environment and Energy Efficiency of Existing Buildings), funded by the Ministry of Science and ICT.

Data Availability Statement: Data are contained within the article.

Conflicts of Interest: The authors declare no conflicts of interest.

References

1. IEA (International Energy Agency). Net Zero by 2050: A Road Map for the Global Energy Sector. 2021. Available online: https://iea.blob.core.windows.net/assets/deebef5d-0c34-4539-9d0c-10b13d840027/NetZeroby2050-ARoadmapfortheGlobalEnergySector_CORR.pdf (accessed on 5 September 2024).
2. IEA (International Energy Agency). Trends in Photovoltaic Applications, Report IEA-PVPS; Volume T1–43. 2024. Available online: https://iea-pvps.org/wp-content/uploads/2024/10/IEA-PVPS-Task-1-Trends-Report-2024.pdf (accessed on 6 November 2024).
3. IEA (International Energy Agency). Categorization of BIPV Applications, Report IEA-PVPS; Volume T15–12. 2021. Available online: https://iea-pvps.org/wp-content/uploads/2021/09/IEA-PVPS-T15-12_2021_BIPV-categorization_report.pdf (accessed on 2 October 2024).
4. Kong, J.; Dong, Y.; Poshnath, A.; Rismanchi, B.; Yap, O. Application of building integrated photovoltaic (BIPV) in net-zero energy building (NEZBs). *Energies* **2023**, *16*, 6401. [CrossRef]
5. Korea Energy Agency New and Renewable Energy Center. Guidelines for Support of New and Renewable Energy Facilities. 2024. Available online: https://www.knrec.or.kr/biz/pds/decree/list.do (accessed on 2 October 2024).
6. IEA (International Energy Agency). Analysis of Requirements, Specifications and Regulation of BIPV, Report IEA-PVPS; Volume T15–08. 2019. Available online: https://iea-pvps.org/wp-content/uploads/2020/01/IEA-PVPS_15_R08__Analysis_of_requirements_specifications_regulation_of_BIPV__report.pdf (accessed on 2 October 2024).
7. Kumari, N.; Singh, S.K.; Kumar, S.; Jadoun, V.K. Performance analysis of partially shaded high-efficiency mono PERC/mono crystalline PV module under indoor and environmental conditions. *Sci. Rep.* **2024**, *14*, 21587. [CrossRef] [PubMed]
8. Shao, C.; Migan-Dubois, A.; Diallo, D. Performance of BIPV system under partial shading condition. *Sol. Energy* **2024**, *283*, 112969. [CrossRef]
9. Ranjan Satpathy, P.; Ramachandaramurthy, V.K.; Roslan, M.F.; Motahhir, S. An adaptive architecture for strategic enhancement of energy yield in shading sensitive building-applied photovoltaic system under real-time environments. *Energy Build.* **2024**, *324*, 114877. [CrossRef]
10. US Department of Energy. Building America Case Study: Photovoltaic Systems with Module-Level Power Electronics, Energy Efficiency & Renewable Energy. 2015. Available online: https://www.nrel.gov/docs/fy15osti/64876.pdf (accessed on 6 November 2024).
11. Deline, C.; Meydbray, J.; Donovan, M. Photovoltaic Shading Test Bed for Module-Level Power Electronics, 2016. Performance Data Update; NREL. Available online: https://www.nrel.gov/docs/fy16osti/62471.pdf (accessed on 2 October 2024).

12. Baumgartner, F.; Vogt, R.; Allenspach, C.; Carigiet, F. Performance analysis of shaded PV module power electronic system. In Proceedings of the 38th European Photovoltaic Solar Energy Conference and Exhibition, Online, 6–10 September 2021; pp. 650–654.
13. Sarwar, S.; Javed, M.Y.; Jaffery, M.H.; Ashraf, M.S.; Naveed, M.T.; Hafeez, M.A. Modular level power electronics (MLPE) based distributed PV system for partial shaded conditions. *Energies* **2022**, *15*, 4797. [CrossRef]
14. Ravyts, S.; Dalla Vecchia, M.; Van den Broeck, G.; Driesen, J. Review on building-integrated photovoltaics electrical system requirements and module-integrated converter recommendations. *Energies* **2019**, *12*, 1532. [CrossRef]
15. Spiliotis, K.; Gonçalves, J.E.; Van De Sande, W.; Ravyts, S.; Daenen, M.; Saelens, D.; Baert, K.; Driesen, J. Modeling and validation of a DC/DC power converter for building energy simulations: Application to BIPV systems. *Appl. Energy* **2019**, *240*, 646–665. [CrossRef]
16. Sutikno, T.; Purnama, H.S.; Widodo, N.S.; Padmanaban, S.; Sahid, M.R. A review on non-isolated low-power DC–DC converter topologies with high output gain for solar photovoltaic system applications. *Clean Energy* **2022**, *6*, 557–572. [CrossRef]
17. Raj, A.; Arya, S.R.; Gupta, J. Solar PV array-based DC–DC converter with MPPT for low power applications. *Renew. Energy Focus* **2020**, *34*, 109–119. [CrossRef]
18. Osmani, K.; Haddad, A.; Lemenand, T.; Castanier, B.; Ramadan, M. An investigation on maximum power extraction algorithms from PV systems with corresponding DC-DC converters. *Energy* **2021**, *224*, 120092. [CrossRef]
19. Eum, J.; Park, S.; Choi, H. A study on the integration of building photovoltaic modules and exterior materials. In Proceedings of the Architectural Institute of Korea Spring Conference, Busan, Republic of Korea, 26–28 April 2023; Volume 43, p. 461.
20. Eum, J.; Park, S.; Choi, H.J. Effects of power optimizer application in a building-integrated photovoltaic system according to shade conditions. *Buildings* **2024**, *14*, 53. [CrossRef]
21. Korea Meteorological Administration (KMA). Past Observation. Available online: https://www.weather.go.kr/w/obs-climate/land/past-obs/obs-by-day.do (accessed on 2 October 2024).

Disclaimer/Publisher's Note: The statements, opinions and data contained in all publications are solely those of the individual author(s) and contributor(s) and not of MDPI and/or the editor(s). MDPI and/or the editor(s) disclaim responsibility for any injury to people or property resulting from any ideas, methods, instructions or products referred to in the content.